

This is the accepted manuscript made available via CHORUS. The article has been published as:

Phase diagram and correlation functions of the two-dimensional dissipative quantum XY model

Changtao Hou and Chandra M. Varma

Phys. Rev. B **94**, 201101 — Published 2 November 2016

DOI: [10.1103/PhysRevB.94.201101](https://doi.org/10.1103/PhysRevB.94.201101)

Phase diagram and quantum-criticality of the two dimensional dissipative quantum XY model

Changtao Hou and Chandra M. Varma

Department of Physics, University of California, Riverside, CA

(Dated: September 29, 2016)

Abstract

The two-dimensional quantum XY model, with Caldeira-Leggett form of dissipation, is applicable to the quantum-critical properties of diverse experimental systems, ranging from the superconductor to insulator transitions, ferromagnetic and antiferromagnetic transitions in metals, to the loop-current order transition in the cuprates. We solve the re-expression of this model in terms of orthogonal topological excitations: vortices and a variety of instantons, by renormalization group methods. The calculations explain the extraordinary properties of the model discovered in Monte-Carlo calculations: the separability of the quantum critical fluctuations (QCF) in space and time, the spatial correlation length proportional to logarithm of the temporal correlation length near the transition from disordered to the fully ordered state, and the occurrence of a phase with spatial order without temporal order. They are intimately related to the flow of the metric of time in relation to the metric of space, i.e. of the dynamical critical exponent z . These properties appear to be essential in understanding the strange metallic phase found in a variety of quantum-critical transitions as well as the accompanying high temperature superconductivity.

The quantum XY (DQXY) model, with Caldeira-Leggett form of dissipation, was introduced [1] to understand the superconductor to insulator transitions in 2 D films as a function of the normal state resistance [2]. The model is of-course directly applicable to quasi-2D metallic ferromagnets with strong XY anisotropy, a realization of which has been found in the quantum-critical region [3]. Quasi-2D metallic anti-ferromagnets, with incommensurate uni-axial order or commensurate planar order also map to the dissipative XY model [4]. Quasi-two-dimensional metals are realized in several Fe-based compounds [5], where superconductivity occurs in a region around the antiferromagnetic quantum-critical point, and in several heavy-fermion compounds [6]. The same model also describes the statistical mechanics of the loop-current order in under-doped cuprates [7]. In such Fe-compounds and heavy-fermions, and in the cuprates, the normal state singular Fermi-liquid properties in the quantum-critical or strange metal region, for example the entropy, the resistivity and the nuclear relaxation rates have the same singular functional dependence on temperature, despite the complete difference in their microscopic models [8]. This encourages one in seeking a common universality class for their statistical mechanics. These diverse interesting problems call for a thorough understanding of the phase diagram and the correlation functions of the DQXY model.

It is well known that the classical XY model in 2D does not belong to the Ginzburg-Landau-Wilson (LGW) class of models for phase transitions which in essence are driven by renormalized spin-waves. The classical transition in the 2D-XY model on the other hand is driven by proliferation of vortices [9, 10]. The kinetic energy in the quantum XY model turns it into a Lorentz-invariant model so that the quantum-transition and the associated critical fluctuations are in the same class as the classical 3D XY model. However, on inclusion of dissipation, the model has a much richer phase diagram [11–13]. The 2D dissipative quantum XY model (DQXY) can be transformed [14, 15] to a model in which the properties are governed by topological excitations - two-dimensional vortices and 'warps'. Warps are instantons of monopole anti-monopole combinations with zero net charge and dipole moment. The order parameter correlation functions discovered by Monte-Carlo calculations and traced to proliferation of warps and vortices [12] are quite unlike the form expected in extensions of the LGW theories to quantum-critical phenomena [16, 17].

The action of the (2+1)D quantum dissipative XY model for the angle $\theta(\mathbf{x}, \tau)$ of fixed-

length quantum rotors at space-imaginary time point (\mathbf{x}, τ) is

$$\begin{aligned}
S = & -K_0 \sum_{\langle \mathbf{x}, \mathbf{x}' \rangle} \int_0^\beta d\tau \cos(\theta_{\mathbf{x}, \tau} - \theta_{\mathbf{x}', \tau}) + \frac{1}{2E_0} \sum_{\mathbf{x}} \int_0^\beta d\tau \left(\frac{d\theta_{\mathbf{x}}}{d\tau} \right)^2 \\
& + \alpha \sum_{\langle \mathbf{x}, \mathbf{x}' \rangle} \int_0^\beta d\tau d\tau' \frac{\pi^2}{\beta^2} \frac{[(\theta_{\mathbf{x}, \tau} - \theta_{\mathbf{x}', \tau}) - (\theta_{\mathbf{x}, \tau'} - \theta_{\mathbf{x}', \tau'})]^2}{\sin^2 \left(\frac{\pi|\tau - \tau'|}{\beta} \right)}, \tag{1}
\end{aligned}$$

$\tau/2\pi$ is periodic in β , the inverse of temperature $1/(k_B T)$. $\langle \mathbf{x}, \mathbf{x}' \rangle$ denotes nearest neighbors. The first term is the spatial coupling term as in classical XY model. The second term is the kinetic energy where E_0 serves as the moment of inertia. The third term describes quantum dissipations of the ohmic or Caldeira-Leggett type [18]. Such a dissipation also comes from the decay of the current fluctuations of the DQXY model to fermions current-current correlations with resistance per square R . In that case $\alpha = 4\pi^2(R_Q/R)$, where $R_Q = h/e^2$ is the quantum of resistance per square. For the alternate form of dissipation, in which the last term in (1) is replaced by a periodic function of the θ 's, the transitions remain in the same class as without dissipation [13, 19]. Also when both forms of dissipation are included, the phase diagram and correlation functions are unchanged from those of the Caldeira-Leggett dissipation alone [13].

The phase diagram [11, 12] for this model is shown in Fig. (1). There are three different phases. There is a transition from the disordered phase, by varying the dissipation parameter α or the parameter $\sqrt{K_0 E_0}$, to a phase with the properties of the ordered phase of the classical 3D-XY model. By increasing $\sqrt{K_0 E_0}$ for small enough α , one has a Kosterlitz-Thouless type 2D-vortex induced transition to a quasi-ordered phase, which is spatially ordered but (1D)-disordered in time. The temporal correlations do not change across this transition. The quasi-ordered phase also orders in time by increasing α to the fully ordered phase. In this paper we use the re-expression of the dissipative quantum XY model in terms of warps and vortices and perform renormalization group calculations, which have some interesting new technical aspects, to reproduce the principal features of the phase diagram and of the essential aspects of the correlation functions discovered in the Monte-Carlo calculations.

In Refs.[14, 15], it is shown that after making a Villain transformation [20] or a duality transformation [21] using the Poisson summation formula, and integrating over the small oscillations or spin-waves, the action is expressed in terms of link variables which are

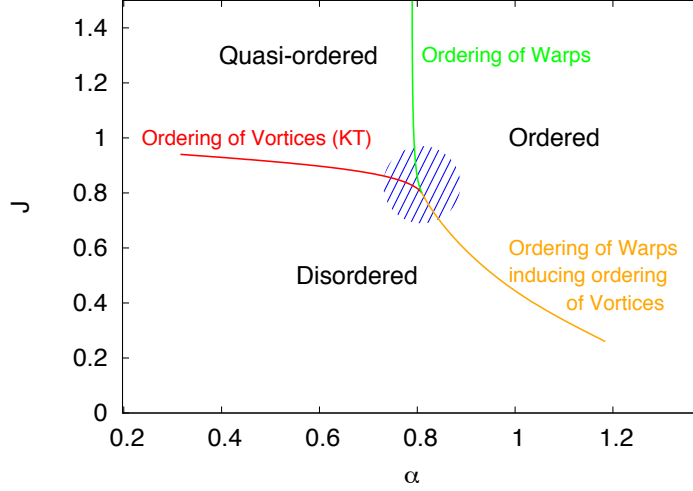


Figure 1. Phase diagram for the dissipative 2D-quantum XY Model calculated by Monte-Carlo in [11, 12]. $J \equiv K_0\tau_c$. The calculations are for a fixed value of the dimensionless variable $E_c \equiv E_0\tau_c = 100$. τ_c^{-1} serves as the ultra-violet cut-off by which K_0 and E_0 of Eq. (1) have been normalized. More results can be found in [12, 13]

differences of θ 's at nearest neighbor sites,

$$m_{\mathbf{x},\mathbf{x}'}(\tau, \tau') \equiv \theta(\mathbf{x}, \tau) - \theta(\mathbf{x}', \tau'). \quad (2)$$

Using Eq. ((2)) at the two nearest neighbors at a lattice site \mathbf{x} , one can define $\mathbf{m}(\mathbf{x})$. Quite generally, $\mathbf{m} = \mathbf{m}_\ell + \mathbf{m}_t$; \mathbf{m}_ℓ , is longitudinal (or curl-free) and \mathbf{m}_t is transverse (or divergence-free). The appearance of \mathbf{m}_ℓ is a novel feature of the quantum dissipative XY-model. As usual

$$\nabla \times \mathbf{m}_t(\mathbf{x}, \tau) = \rho_v(\mathbf{x}, \tau)\hat{\mathbf{z}}, \quad (3)$$

so that $\rho_v(\mathbf{x}, \tau)$ is the charge of the vortex at (\mathbf{x}, τ) . The model also has quantized jumps in phase at the point \mathbf{x} between τ and $\tau + d\tau$. Such jumps produces divergences in \mathbf{m} [15] and can be represented by

$$\frac{\partial \hat{\nabla} \cdot \mathbf{m}_\ell(\mathbf{x}, \tau)}{\partial \tau} = \rho_w(\mathbf{x}, \tau). \quad (4)$$

Although a continuum description is being used for simplicity of writing, it is important to do the calculation so that the discrete nature of the ρ_v, ρ_w fields is always obeyed. The action of the model (1) in terms of warps and vortices, after Fourier-transforming from the result given in [14, 15] is,

$$\begin{aligned} S = & \frac{J}{2\pi} \sum_{i \neq j} \rho_v(r_i, \tau_i) \ln \frac{|r_i - r_j|}{a_c} \rho_v(r_j, \tau_j) + \alpha \sum_{i \neq j} \rho_w(r_i, \tau_i) \ln \frac{|\tau_i - \tau_j|}{\tau_c} \rho_w(r_i, \tau_j) \\ & + g \sum_{i \neq j} \rho_w(r_i, \tau_i) \frac{1}{\sqrt{|r_i - r_j|^2 + v^2(\tau_i - \tau_j)^2}} \rho_w(r_j, \tau_j) + \ln y_w \sum_i |\rho_w(r_i, \tau_i)|^2 + \ln y_v \sum_i |\rho_v(r_i, \tau_i)|^2. \end{aligned} \quad (5)$$

The sum is over all space points and over imaginary time τ from an upper cut-off τ_c to $1/(2\pi T)$. Here $J = K_0 \tau_c, g = \sqrt{J/E_c}/4\pi, v^2/c^2 = JE_c, E_c = E_0 \tau_c$ are dimensionless variables, and $c = a/\tau_c$, a is the lattice constant. Some spatial dimensions have been absorbed in the re-definition of ρ_v and ρ_w [15]. The first term in (5) is the action of the *classical* vortices interacting with each other through logarithmic interactions in space but the interactions are local in time. The second term describes the warps interacting logarithmically in time but locally in space. The third term is the action for a (anisotropic) Coulomb field between warps, which if present alone for the isotropic case is known [22] not to cause a transition; it will be seen to play a crucial role in the present problem in which the space-time anisotropy is required to flow. The short distance core-energy of the warps and vortices is taken care of by the final term in which y_v and y_w are the fugacity of the vortices and the warps, respectively.

The warp and the vortex variables in the first two terms are orthogonal since they are related respectively to the divergence and rotation of a vector field. The problem is trivial with just these two terms alone. If the first term dominates, one expects a transition of the class of the classical Kosterlitz-Thouless transition through the renormalization of the fugacity of vortices to 0. But the ordered phase would have bound vortex-anti-vortex pairs in space with nothing to correlate them in time. If the second term dominates, there is a quantum transition to a phase with binding of warp-antiwarp pairs in time but nothing to

order them with respect to each other in space. Four distinct phases would therefore be found in the $\alpha - JE_c$ plane. This is unlike the phase diagram of Fig. (1). We will show that given the growth of correlations due to the renormalization of the fugacity of vortices or of warps, the flow to the critical points are determined by the third term, which scales time and space differently, depending on whether the warps or the vortices in the first two terms dominate, i.e. by the relative magnitudes of J and α . This leads to ordering at $T = 0$ both in time and space to a state with symmetry of the 3D XY model over most of the phase diagram but an interesting region in which the system is spatially ordered for small times but disordered at larger times persists.

The renormalization group (RG) equations for the coupling J and the vortex fugacity y_v may be obtained following the procedure of Kosterlitz [23] or Jose et al.[21]. The renormalization of these quantities obtained by scaling the spatial length scale $\ell_r = \ln(r/a)$, where the lattice constant a serves as the short-distance cut-off are,

$$dJ = -\pi y_v^2 J^2 d\ell_r; \quad dy_v = (2 - \frac{J}{4\pi}) y_v d\ell_r. \quad (6)$$

To derive the RG equation for the parameters for the warps, we consider the effective interaction between two warps at a point in space and separated by time $\tau > \tau_c$ as modified by the screening due to the creation of a virtual pair, at times τ' and τ'' , $\tau_c < |\tau' - \tau''| < \tau_c e^{d\ell_\tau}$, where $\ell_\tau = \ln(\tau/\tau_c)$ and τ_c is the short-time cutoff. The RG equations for α by scaling ℓ_τ is derived. However the fugacity of warps is renormalized by both rescaling ℓ_τ and, due to the third term in the action (5), by rescaling ℓ_r . Therefore we must also consider the renormalization of the parameters g and v . A scale dependent $v = d|r|/d\tau$ is equivalent to allowing a scale-dependent dynamical critical exponent, $z \equiv d\ell_\tau/d\ell_r$.

The renormalization procedure is given in a supplementary section. The results are

$$d\alpha = -2\alpha y_w^2 d\ell_\tau, \quad (7)$$

$$dy_w = y_w((1 - \alpha)d\ell_\tau + (2 - g)d\ell_r), \quad (8)$$

$$dg = -gd\ell_r - \frac{8\pi^3}{3} \frac{g^2 y_w^2}{a_c} \left(\left(\frac{1}{4v} + \frac{v}{2} \right) d\ell_\tau + \left(\frac{1}{v} + \frac{v}{3} \right) d\ell_r \right), \quad (9)$$

$$dv = (d\ell_\tau - d\ell_r)v. \quad (10)$$

These equations may be written as scaling equations either with respect to ℓ_r or ℓ_τ by suitably using z . It is also redundant to keep both z and v . We note the identity

$$\frac{dz^{-1}}{d\ell_\tau} - z^{-1}(1 - z^{-1}) = \frac{\tau}{r} \frac{dv}{d\ell_\tau}. \quad (11)$$

Using this, (10) can be re-written as

$$\frac{d(z^{-1})}{d\ell_\tau} = 2z^{-1}(1 - z^{-1}). \quad (12)$$

We now have a closed system of RG equations. First, we note that Eq. (12) gives the fixed points $z^* = 1, \infty, 0$. $z^* = 1$ is a stable fixed point. The $z^* = 1$ fixed point corresponds to stable fixed point at its initial value. The $z^* = \infty$ fixed point is unstable corresponding to the unstable fixed point for velocity at $v^* = \infty$. The $z^* = 0$ fixed point is also unstable corresponding to the unstable fixed point at $v^* = 0$. These results are in accord with the investigations on expansion about isotropy of the classical anisotropic coulomb gas model in 3D [24], i.e. the model with only the third term in (5). We find that the 2D limit, (i.e. $v^* = 0$) as well as the 1D limit ($v^* = \infty$) is unstable (i.e. has a critical point) towards the stable isotropic problem.

We now consider the regimes of initial parameters in which the three different regions in the phase diagram in Fig.(1) are obtained, and calculate the correlation lengths in time and space about the critical points separating them:

I. $J/2\pi \lesssim 4, \alpha \lesssim 1$: On examining the first two terms of the transformed action, (5), or the RG equations (6, 7, 8), one finds, as will be shown below that the fugacity of both vortices and warps is large in this region, provided $g < 2$. The model is therefore in its quantum disordered state in this region, as in the phase diagram in Fig.(1).

II. $J/2\pi \lesssim 4$ and $\alpha \approx 1$: In this region, we must first analyze the equations for the warps, Eqs.(7, 8, 9). We note from Eqs. (7, 8) that for $z^* \rightarrow \infty$, and the initial $\alpha > 1$, α and y_w flow asymptotically for long times $\rightarrow 0$, provided g remains finite. For initial $\alpha < 1$, α flows asymptotically at long times to 0 and y_w to ∞ . So $\alpha^* = 1$ is an unstable critical point. We note from (9) that near the $\alpha^* = 1$ fixed point, as $z \rightarrow \infty$ and $y_w \rightarrow 0$, g flows to a constant value, consistent with the above requirement.

We expand near the unstable $\alpha = 1^-$ fixed point and solve, to find

$$y_w \propto (e^{-\tau/\xi_\tau} - 1); \quad \xi_\tau \propto e^{(b_0/(1-\alpha))^{12}}. \quad (13)$$

b_0 is a coefficient of $O(1)$. To study J and y_v near this point, we write the scaling equations in terms of ℓ_τ by using $z \equiv d\ell_\tau/d\ell_r$. The flow of the vortex parameters J and y_v is now given by

$$\frac{dJ}{d\ell_\tau} = -\frac{1}{z}\pi y_v^2 J^2, \quad \frac{dy_v}{d\ell_\tau} = \frac{1}{z}\left(2 - \frac{J}{4\pi}\right)y_v. \quad (14)$$

We also have

$$\frac{dy_v}{dy_w} = \frac{1}{z(1-\alpha)}\left(2 - \frac{J}{4\pi}\right)\frac{y_v}{y_w}. \quad (15)$$

Near the critical point $z^* \rightarrow \infty$, but $(1-\alpha) \rightarrow 0$. But, near this point, $1/z = 0 + O(\tau^{-2})$ and α approaches its fixed point of 1 exponentially slowly with τ^{-1} . Therefore, if $(2 - J/4\pi)$ does not flow, as is found self-consistently,

$$y_v \propto y_w^{1/z}, \text{ i.e. for } z \rightarrow \infty, y_v \propto \ln y_w. \quad (16)$$

We can get a correlation length in space from the relation $d\ell_r = (1/z)d\ell_\tau$ and the result that $1/z \propto \tau^{-2}$ near this fixed point. This gives the important result that spatial correlation length ξ_r and the temporal correlation length ξ_τ are related by

$$\frac{\xi_r}{a} \propto \log\left(\frac{\xi_\tau}{\tau_c}\right). \quad (17)$$

The same results for the RG flows are also obtained from the numerical solution of the equations near this critical point. The critical point corresponds to the quantum-disordered to 3D ordered transition in Fig.(1). The correlation lengths in time and space deduced above have been found in extensive Monte-carlo calculations [12]. We understand now that the physical reason of the conjecture made in [12, 25] that the freezing of warps drives the freezing of vortices. Specifically, the growing fugacity of warps drives a flow of the space-time metric parameter z so that the fugacity of the vortices, Eq. (14) becomes scale-dependent even for values of J below the value of 8π .

III. $\alpha \lesssim 1$ and $J/4\pi \approx 2$: In this region, it is appropriate to start the analysis with examination of Eqs. (6) for flow of J and y_v . Eqs. (6) have the standard KT flow with the KT point $J^* = 8\pi$ near which $y_v \rightarrow 0$. For $J > 8\pi$, y_w flows towards ∞ and J flows to ∞ . Following Nelson and Kosterlitz, the spatial stiffness has a jump at the transition. Now we examine whether this is changed by the action of warps. We start by assuming that such a fixed point corresponds to the $z \rightarrow 0$ unstable fixed point, which is the same as $v \rightarrow 0$. Let

us study how warps are affected by this. Eq. (9) gives that g flows to 0. The equations (7), (8) should now be written in terms of the scale length ℓ_r as

$$\frac{d\alpha}{d\ell_r} = -2z\alpha y_w^2; \quad \frac{dy_w}{d\ell_r} = y_w(z(1-\alpha) + 2). \quad (18)$$

We see that neither the fugacity y_w nor α flows in this case. So warps remain completely unaffected by the vortex freezing. The time dependence of the correlation remains unaffected, as can be checked directly. This is consistent with the assumption that this fixed point corresponds to $z^* = 0$. This corresponds to the transition from the quantum-disordered phase to the quasi-ordered phase in Fig. (1), in which the spatial correlations are those of the ordered Berezinsky-Kosterlitz-Thouless phase, with a jump of spatial stiffness at the transition. But the correlations in time remain of the disordered phase, consistent with the Monte-carlo calculations.

IV. $J/2\pi \gtrsim 4, \alpha \rightarrow 1^-$: As discussed in III, for these values of J , $y_v \rightarrow \infty$ and isolated vortices are frozen for $\alpha < 1$. As $\alpha \rightarrow 1^-$, y_v remains stable at this value and the RG equations for α and y_w are simply (7) and (8), respectively. So $y_w \rightarrow 0$ as $\alpha \rightarrow 1$ and density of isolated warps tends to 0 rapidly for $\alpha > 1$. For $\alpha > 1$, long-range correlations develop in time as well as space and the ordered state is similar to that obtained directly from the quantum disordered state discussed in II above.

V. $\alpha \gtrsim 1$: In this case, y_w increases, which forces the flow of α towards 0. But the RG calculation, as is well known, is uncontrolled because the stable fixed point is of the strong-coupling kind. The $z \rightarrow \infty, \alpha \rightarrow 1^-$ critical point is unstable towards the stable fixed point $z \rightarrow 1, \alpha \rightarrow 0$.

In a supplementary section, we derive the correlation functions of the order parameter, using the results of RG equations above, and a simple generalization of the procedures used earlier [25] which are themselves a space-time generalization of the procedure of Ref. [21]. We find the remarkable result that the correlation function of the order parameter is separable in space and time. Near the critical point $z^* = \infty$ and $\alpha \rightarrow 1$, the correlation function is

$$C(\mathbf{r} - \mathbf{r}', \tau - \tau') \equiv \langle \cos \theta(\mathbf{r}, \tau) \cos \theta(\mathbf{r}', \tau') \rangle \propto \log(|\mathbf{r} - \mathbf{r}'|) e^{-\frac{|\mathbf{r} - \mathbf{r}'|}{\xi_r}} \frac{1}{|\tau - \tau'|} e^{-\frac{|\tau - \tau'|}{\xi_\tau}}. \quad (19)$$

The Fourier transform of its imaginary part is

$$ImC(\omega, \mathbf{q}) \propto \frac{1}{\kappa_q^2 + q^2} \tanh\left(\frac{\omega}{\sqrt{4T^2 + \kappa_\omega^2}}\right); \kappa_q \approx 1/\xi_r, \quad \kappa_\omega \approx 1/\xi_\tau. \quad (20)$$

and with the result derived above that $(\xi_r/a) \propto \log(\xi_\tau/\tau_c)$, and with a high frequency cut-off $\omega_c = \tau_c^{-1}$.

The principal features of the phase diagram in Fig. (1) and the correlation functions found by Monte-Carlo calculations are obtained by the RG calculations above. The extraordinary features of the results are understood as arising from the fact that the transitions are driven by orthogonal topological excitations, vortices and warps, which are respectively local in time and in space and the flow of the dynamical critical exponent z between its critical values $z^* = 0, \infty$ at the unstable fixed points and from them to the stable $z^* = 1$ critical point. Some details of the phase diagram and of the correlations are not obtained in leading order RG. The transition from the disordered to the 3D-XY ordered state occurs in RG calculations at $\alpha = 1$, while in Monte-Carlo calculations, the ordered phase requires larger α for smaller JE_c . The Monte-Carlo calculations reveal that the transition from the quantum-disordered phase to the ordered phase occurs along a line in the $J - \alpha$ plane, whereas the leading order RG results give the transition to be at $\alpha = 1$ for all $J < 8\pi$. In the Monte-carlo calculations, it is found also that for fixed α , the correlation length ξ_τ varies as $(g - g_c)^{-\nu_\tau}$, with $\nu_\tau \approx 0.5$, and again with $(\xi_r/a) \propto \log(\xi_\tau/\tau_c)$. It should also be mentioned that the transformation to the topological model relies on a finite dissipation coefficient α . One cannot take the limit $\alpha \rightarrow 0$ and get the properties of the (2+1) D quantum XY model without dissipation. The passage of the properties of the model from that of the 3D classical XY model at $\alpha = 0$ to those at finite α has been investigated by Monte-Carlo calculations [13].

The present theory provides the microscopic basis for the results derived from the form of the critical fluctuations hypothesized long ago to get the marginal fermi-liquid [26]. The frequency dependence is identical to that proposed earlier but the momentum dependence in Eq. (20) removes the assumption of spatial locality with $\xi_r \propto \log \xi_\tau$. As shown in Refs. [8], the results for transport and thermodynamic properties derived earlier follow from scattering of fermions by such fluctuations with a vertex proportional to q , which has also been derived. The fluctuations in Eq. (20) themselves have been directly observation in cuprates in the long wave-length limit by Raman scattering, [27] and have been deduced, by analyzing high resolution ARPES data, over a large region of momentum space as responsible for their strange metal properties as well as promotion of d-wave superconductivity [28]. Analysis of the limited data on fluctuations near antiferromagnetic critical point in a heavy fermion

compound [29] and in an iron compound [30] has been found consistent [31] with Eq. (20). More experiments are suggested.

Acknowledgements: We gratefully acknowledge very useful discussions with Vivek Aji and H. Krishnamurthy. This work was partially supported by NSF under the grant DMR 1206298.

-
- [1] S. Chakravarty, G. Ingold, S. S. Kivelson, and G. Zimanyi, Phys. Rev. B **37**, 3283 (1988).
 - [2] N. J. Lin, Yen-Hsiang and A. Goldman, Physica C **514**, 130 (2015).
 - [3] L. Wua, M. Kima, K. Parks, A. Tsvelik, and M. Aronson, PNAS **39**, 14088 (2014).
 - [4] C. M. Varma, Phys. Rev. Lett. **115**, 186405 (2015).
 - [5] K. Ishida, Y. Nakai, and H. Hosono, J. Phys. Soc. Jpn. **78**, 062001 (2009).
 - [6] H. Löhneysen, A. Rosch, M. Vojta, , and P. Wölfle, Rev. Mod. Phys. **79**, 1015 (2007).
 - [7] C. M. Varma, Phys. Rev. B **73**, 155113 (2006).
 - [8] C. M. Varma, Rep. Prog. Phys. **79**, 082501 (2016).
 - [9] J. Kosterlitz and D. Thouless, J. Phys. C **6** (1973).
 - [10] V. Berezinskii, Zh. Eksp. Teor. Fiz. **59**, 907 (1970).
 - [11] E. B. Stiansen, I. B. Sperstad, and A. Sudbø, Phys. Rev. B **85**, 224531 (2012).
 - [12] L. Zhu, Y. Chen, and C. M. Varma, Phys. Rev. B **91**, 205129 (2015).
 - [13] L. Zhu, C. Hou, and C. M. Varma, arXiv:1604.01111 (2016).
 - [14] V. Aji and C. M. Varma, Phys. Rev. Lett. **99**, 067003 (2007).
 - [15] V. Aji and C. M. Varma, Phys. Rev. B **82**, 174501 (2010).
 - [16] T. Moriya, *Spin Fluctuations in Itinerant Electron Magnetism* (Springer-Verlag, Berlin, 1985).
 - [17] J. A. Hertz, Phys. Rev. B **14**, 1165 (1976).
 - [18] A. Caldeira and A. Leggett, Ann. Phys. (NY) **149**, 374 (1983).
 - [19] I. B. Sperstad, E. B. Stiansen, and A. Sudbø, Phys. Rev B **84**, 180503 (2011).
 - [20] J. Villain, J. Phys. (Paris) **36**, 581 (1975).
 - [21] J. Jose, L. L. P. Kadanoff, S. Kirkpatrick, and D. Nelson, Phys. Rev. B **16**, 1217 (1977).
 - [22] A. Polyakov, Nucl. Phys. B **120**, 429 (1977).
 - [23] J. Kosterlitz, J. Phys. C **7**, 1046 (1974).
 - [24] J. M. Kosterlitz, J. Phys. C **10**, 3753 (1977).

- [25] V. Aji and C. M. Varma, Phys. Rev. B **79**, 184501 (2009).
- [26] C. M. Varma, P. B. Littlewood, S. Schmitt-Rink, E. Abrahams, and A. E. Ruckenstein, Phys. Rev. Lett. **63**, 1996 (1989).
- [27] F. Slakey, M. V. Klein, J. P. Rice, and D. M. Ginsberg, Phys. Rev. B **43**, 3764(R) (1991).
- [28] J. M. Bok and et al., Science Advances **2**, e1501329 (2016).
- [29] A. Schröder and et al., Phys. Rev. Lett. **80**, 5623 (1998).
- [30] D. S. Inosov, J. T. Park, P. Bourges, D. L. Sun, Y. Sidis, A. Schneidewind, K. Hradil, D. Haug, C. T. Lin, B. Keimer, and V. Hinkov, Nature Phys. **6**, 178 (2010).
- [31] C. M. Varma, L. Zhu, and A. Schroeder, Phys. Rev. B **92**, 155150 (2015).